Crater formation in gold nanoislands due to MeV self-ion irradiation

P. V. Satyam,[a] J. Kamila,[b] S. Mohapatra, B. Satpati, D. K. Goswami, and B. N. Dev
Institute of Physics, Sachivalaya Marg, Bhubaneswar-751 005, India

R. E. Cook, Lahsen Assoufid, and J. Wang
Argonne National Laboratory, 9700 South Cass Avenue, Argonne, Illinois 60439

N. C. Mishra
Department of Physics, Utkal University, Bhubaneswar-751 004, India

(Received 8 October 2002; accepted 3 March 2003)

The modification of gold nanoislands, grown on silicon substrates under high-vacuum conditions, by MeV self-ion irradiation has been studied by using scanning electron microscopy, transmission electron microscopy, atomic force microscopy, and x-ray reflectivity. Upon irradiation with 1.5 MeV Au^{2+}, two types of craters are observed on the Au islands: Empty craters and craters with a central hillock. The contribution of plastic flow, pressure spike, and sputtering to the crater formation during the ion impacts on the gold islands is analyzed. Thermal spike confinement within the gold islands is also proposed to be one of the possible reasons for crater formation in nanoislands. © *2003 American Institute of Physics.* [DOI: 10.1063/1.1569026]

Ion irradiation in materials has been extensively studied for many years due to its significant technological importance in the microelectronics industry. A radiation damage model that explains the production of interstitial atoms, vacant lattice sites, and displacement spikes was introduced a few decades ago.[1] The composition and morphology modification due to the thermal spike was investigated both experimentally[2–9] and theoretically.[10–19] Surface modification of materials by energetic charged particles yielded a variety of features: Hillocks,[9,16] craters,[2–19] etc. Recently, Birtcher *et al.*[3–6] reported the formation of craters and their annihilation and ejection of nanoparticles from Au films that were irradiated with 50–400 keV Xe ions, providing evidence for the independence of pulsed plastic flow on the material structure. The formation of holes in gold thin foils as a result of single-ion impacts by 200 keV Xe ions has been explained by the plastic flow of material on the order of tens of thousands of Au atoms per ion impact. Plastic flow as a consequence of individual ion impacts, results in the filling of both holes and craters, as well as thickening of the gold foil.[6]

Recently, the application of ion beams to modify nanomaterial properties has become an important topic in the areas of nanofabrication and nanosciences. Due to athermal processes involved in ion irradiation, modifying the properties of these materials may be feasible to an extent not possible by conventional methods.[20–22] When irradiation was performed at an angle of 45° with respect to the Si substrate surface, MeV Au irradiation induces an anisotropic plastic deformation turning spherical colloids into ellipsoidal shapes. This observation supports the thermal spike model of anisotropic deformation.[21] In the present work, we report crater formation in gold nanoisland structures due to MeV self-ion irradiation and propose the possibility of confinement of the thermal spike in nanoislands.

Most of the molecular-dynamics calculations are performed in the low-energy regime (for incident ion energy <200 keV), where crater formation has been related to the melting temperature and the cohesive energy. Nordlund *et al.*[18] reported that the size of craters produced by energetic ion and cluster ion impact scales with the inverse of the product of the melting temperature and cohesive energy when other material parameters are the same, and they proposed that the flow of liquid produced by ions was the reason for the different behavior of macroscopic and ion-induced cratering. Molecular-dynamics simulations of low-energy (50 keV) self-bombardment of copper and nickel resulted in observation of collective displacement of atoms.[10] The high pressures developed in collision cascades centered well below the surface can cause a coherent displacement of thousands of atoms over tens of atomic planes and can result in shear-induced slip motion towards the surface.[10] To our knowledge, no theoretical simulation has been performed for a system where the thermal spike is confined to nanometer regions. Our results provide the experimental data for understanding crater formation on these nanoislands.

There are several studies of MeV ion interaction on thin films.[23–25] Andersen *et al.*[23] observed a rapid degradation of discontinuous gold films on 15–23 nm thick carbon substrates when they were irradiated with MeV N, O, F, Cl, and Br ions up to fluences of 5×10^{15} ions cm^{-2} and fluxes up to 8×10^{11} ions $cm^{-2}\,s^{-1}$. In the case of a relatively thick Au film (60–80 nm thick), surface craters were observed for Bi^{+} and Bi^{2+} bombardment in the energy range of 10–500 keV.[2] Nanoparticles were ejected when a thick Au film (of thickness 62 nm) was irradiated with 400 keV Xe ions at fluence rates between 1 and 2×10^{11} ions $cm^{-2}\,s^{-1}$, and while the total fluence was kept to less than 1×10^{14} ions cm^{-2}. Changes in morphology during the Xe ion irradiation were attributed to a localized, thermal-spike-induced melting,

[a]Author to whom all correspondence should be addressed; electronic mail: satyam@iopb.res.in
[b]Present address: B.J.B. Jr. College, Bhubaneswar, India.

coupled with plastic flow under the influence of surface forces.[3–6] Several interesting studies have been published on heavy-ion-induced grain growth in elemental and homogeneous alloy films where grain growth is also described by a thermal-spike model in which irradiation-induced cylindrical spikes thermally activate atom jumps resulting in boundary migration.[23–25] It would be interesting to see the effects related to thermal spike for isolated nanograins, where a possibility of confinement could be seen. This requires a heavy-ion irradiation on high-atomic-number elements. One such possibility is to have gold nanoislands irradiated with energetic gold ions.

In the present study, Au films of thickness about 2 nm were deposited by evaporation under high-vacuum conditions ($\approx 2\times10^{-6}$ Torr) onto Si(100) substrates at room temperature. Prior to the deposition, the substrates were cleaned (rinsed) with deionized water followed by rinsing in methanol, trichloroethelene, methanol, and a final rinse in deionized water. The native oxide was not etched. The Au deposition rate was $\approx 0.1\ \mathrm{nm\,s^{-1}}$. The irradiation was carried out with 1.5 MeV Au^{2+} ions into the Au films kept at room temperature at the ion-implantation beamline at the 3.0 MV tandem Pelletron accelerator at the Institute of Physics, Bhubaneswar, India.[26] The implantation was performed at an angle of 60° between the sample surface and the ion beam. The fluence rates were between 1.1×10^{11}–$1.6\times10^{11}\ \mathrm{ions\,cm^{-2}\,s^{-1}}$. The total fluence on the samples varied from 5×10^{13}–$1\times10^{15}\ \mathrm{ions\,cm^{-2}}$. Transmission electron microscopy (TEM) measurements were carried out with 200 keV electrons (2010 UHR JEOL) also at the Institute of Physics, Bhubaneswar, India. Scanning electron microscopy (SEM) measurements were carried out using 4.0 keV electrons in an Hitachi S-4700-II (Field-emission gun-SEM) at the Electron Microscopy Center of the Materials Science Division, Argonne National Laboratory (ANL), Illinois. The atomic force microscopy (AFM) measurements were carried out at the Metrology Laboratory, Advanced Photon Source (APS), Argonne National Laboratory using a Topo Metrix Explorer AFM. The x-ray reflectivity measurements were performed at 1-BM beamline of Synchrotron Radiation Instrumentation-Collaborative Access Team, APS, ANL.

Secondary electron images of irradiated gold nanoisland specimens at fluences of 5×10^{13}, 1×10^{14}, 5×10^{14}, and $1\times10^{15}\ \mathrm{ions\,cm^{-2}}$ are shown in Fig. 1. At a thickness of ≈ 2 nm of Au, isolated Au nanoislands are formed on Si, because of the nonwetting nature of Au on Si. On the pristine films, the size of the islands is distributed in a range of 10–30 nm. From Figs. 1(c) and 1(d), one can observe the increase of island size from 10 nm to 60 nm as fluence varies from 1×10^{14} to $1\times10^{15}\ \mathrm{ions\,cm^{-2}}$. Also, three types of islands are observed: (i) islands with interior gray levels that are slightly less than the island walls [prominent in Fig. 1(c)], (ii) islands with interior gray levels that are similar to the area outside the islands [prominent in Fig. 1(d)], and (iii) smaller islands (or hillocks) which can be seen as white dots [prominent in Fig. 1(d)]. We refer to the type of islands mentioned in (i) and (ii) as craters without hillocks and (iii) as craters with hillocks. The increase in the size of the islands can be explained due to flow of Au upon irradiation onto the surface, and then the gold material spreads over the sides of island by the surface tension.[3–6,11] The Rutherford backscattering measurements on similar set of samples were carried out to determine the loss of gold due to sputtering. These results clearly show that sputtering takes place and hence there is no conservation of gold in the islands before and after the irradiation. So, the volumes of the islands will not remain same. In a modified 60 nm island [(i) and (ii) cases], the width of the crater is about ≈ 23 nm. The crater formation could be clearly seen at a fluence of 5×10^{14}. With a higher fluence of $1\times10^{15}\ \mathrm{ions\,cm^{-2}}$, no appreciable change in the crater size occurs. Sizes were measured using line profiles across the islands.

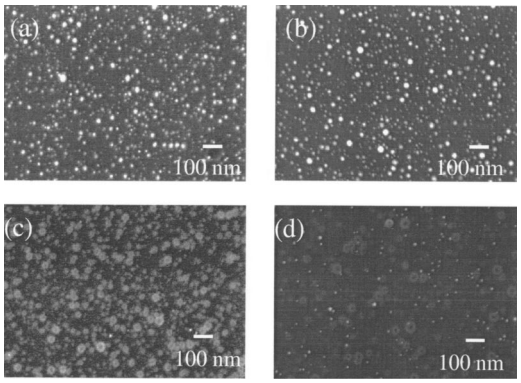

FIG. 1. SEM image of 1.5 MeV Au^{2+} irradiated on gold nanoislands. Fluence: (a) $5\times10^{13}\ \mathrm{ions\,cm^{-2}}$, (b) $1\times10^{14}\ \mathrm{ions\,cm^{-2}}$, (c) $5\times10^{14}\ \mathrm{ions\,cm^{-2}}$, and (d) $1\times10^{15}\ \mathrm{ions\,cm^{-2}}$. (c) and (d) Formation of craters.

The AFM measurements were done on a sample irradiated with $5\times10^{14}\ \mathrm{ions\,cm^{-2}}$ (Fig. 2). Two main features in the surface morphology can be seen: Empty craters and craters with central hillocks. These features provide an explanation for contrast in the SEM crater images in Figs. 1(c) and 1(d). From the AFM measurements, the average diameter of empty craters (islands with craters and no hillocks) is ≈ 60 nm and the depth is ≈ 2 nm. For craters with hillocks, the average crater diameter is ≈ 52 nm, the depth is ≈ 0.45 nm, the hillock diameter is ≈ 10 nm and the hillock height is ≈ 0.15 nm.

The TEM measurements were carried out on a $1\times10^{14}\ \mathrm{ions\,cm^{-2}}$ sample. The TEM micrographs in Fig. 3 were recorded at different tilt angles, and then the images were added (stereomicroscopy) for better contrast. Although the crater structure cannot be observed in the SEM images of the sample irradiated with the $1\times10^{14}\ \mathrm{ions\,cm^{-2}}$ fluence, possibly due to limited spatial resolution, the TEM images

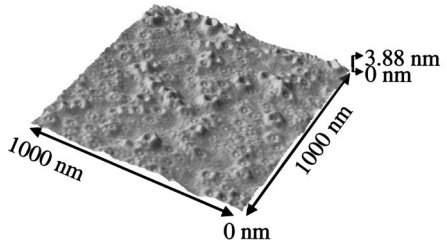

FIG. 2. AFM measurements on the specimen irradiated with $5\times10^{14}\ \mathrm{ions\,cm^{-2}}$.

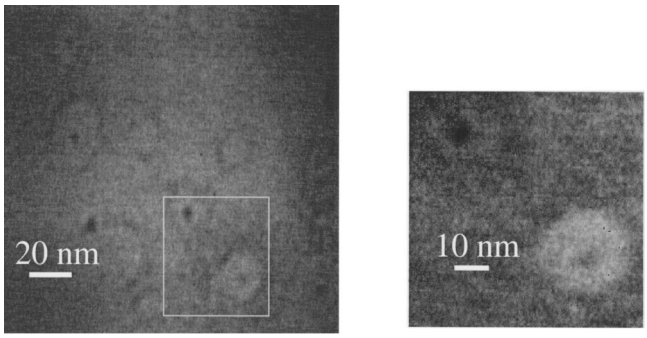

FIG. 3. Defocused TEM image of craters: (a) image taken at one tilt angle, and (b) addition of two raw images from the area enclosed within the box in (a) taken at two different tilt angles at the same defocus condition. The contrast improves significantly by the addition procedure.

clearly show the formation of both types of craters, with and without hillocks. To collect the TEM images, the planar samples were prepared using low-energy 3.0 keV Ar ion milling using GATAN PIPS equipment.[27] X-ray reflectivity results show evidence for the loss of Au as would be expected to happen due to the ion irradiation (data not shown). Also, the surface roughness increases with increase of ion fluence.

In experiments carried out on gold films, Birtcher *et al.*[3–6] have identified plastic flow processes associated with individual impacts. Our observation can be explained on the basis of confinement of thermal spikes within gold nanoislands because the neighboring material is silicon. Birtcher *et al.*[3–6] also observed a 2%–5% probability for crater production in continuous films due to single-ion impacts. We are not doing single-ion measurements as discussed in the work of Birtcher *et al.*[3–6] At a fluence of 1×10^{14} ions cm^{-2}, there will be about 1 ion per nm^{+2}. As our nanoislands are bigger in area (typically 100 to 900 nm^2), the effects of multiple ions impinging on one island for fluences $\geqslant 1\times10^{14}$ ions cm^{-2} have to be considered. The total probability for crater formation at a given fluence is discussed here. As obtained by SEM and AFM on 5×10^{14} ions cm^{-2} samples, the probability for obtaining craters with hillocks is about $\approx 32\%$. Obtaining an accurate count of craters without hillocks from SEM images was difficult, but an approximate probability for crater production without hillocks is 30%. The AFM data from the same sample yield a probability of about 12% for craters without hillocks. Although SEM and AFM results are in agreement with respect to the formation of craters with hillocks, the total probability of crater formation was measured to be 60% by SEM and 44% by AFM. In the case of 1×10^{15} ions cm^{-2}, the SEM results show about 15% of craters with hillocks and some small island structures. The probability of the production of craters is determined by comparing the number of hillocks and craters in a specified area as a function of fluence. Reduction in the probability of crater formation could be due to the annihilation of craters, as described by Birtcher *et al.*[3–6] Smaller islands which are seen as white dots in Fig. 1(d) are possible as a consequence of the annihilation of craters. One can also see the lower number of craters in the work of Merkle *et al.*[2] We speculate that this higher probability of crater production in our samples when compared to a thin continuous film sample[2–6] is possible due to the confinement of the thermal spike within the nanoislands. Though SEM results do not show any crater production for the 1×10^{14} ions cm^{-2} sample, TEM measurements show about 40% crater production. Further studies having more control of parameters like particle size and current density-simulating single-ion impacts on the isolated nanoislands are planned. We conclude that MeV self-ion irradiation in gold nanoislands has resulted in providing evidence for thermal-spike confinement. Also, this work may generate interest in the theoretical simulations of thermal-spike confinement.

The use of the Advanced Photon Source and the Electron Microscopy Center at Argonne National Laboratory was supported by the U. S. Department of Energy, Office of Basic Energy Sciences, under Contract No. W-31-109-ENG-38. One of the authors (P.V.S.) would like to thank APS, ANL for the support for his visit of APS when part of the experiment was performed.

[1] J. A. Brinkman, Am. J. Phys. **24**, 246 (1956).
[2] K. L. Merkle and W. Jager, Philos. Mag. A **44**, 741 (1981).
[3] R. C. Birtcher, J. Matsuo, and I. Yamada, Nucl. Instrum. Methods Phys. Res. B **175**, 36 (2001).
[4] R. C. Birtcher, S. E. Donnelly, and S. Schlutig, Phys. Rev. Lett. **85**, 4968 (2000).
[5] S. E. Donnelly and R. C. Birtcher, Phys. Rev. B **56**, 13599 (1997).
[6] R. C. Birtcher and S. E. Donnelly, Phys. Rev. Lett. **77**, 4374 (1996).
[7] R. M. Papaleo, L. S. Farenzena, M. A. de Araujo, R. P. Livi, M. Alurralde, and G. Bermudez, Nucl. Instrum. Methods Phys. Res. B **148**, 126 (1999).
[8] L. S. Farenzena, R. P. Livi, M. A. de Araujo, G. Garcia Bermudez, and R. M. Papaleo, Phys. Rev. B **63**, 104108 (2001) and references therein.
[9] C. Teichert, M. Hohage, T. Michely, and G. Comsa, Phys. Rev. Lett. **72**, 1682 (1994).
[10] K. Nordlund, J. Keinonen, M. Ghaly, and R. S. Averback, Nature (London) **398**, 49 (1999).
[11] S. Averback, Phys. Rev. Lett. **72**, 364 (1994).
[12] E. M. Bringa, K. Nordlund, and J. Keinonen, Phys. Rev. B **64**, 235426 (2001).
[13] Q. Yang, T. Li, B. V. King, and R. J. MacDonald, Phys. Rev. B **53**, 3032 (1996).
[14] T. Diaz de la Rubia, R. S. Averback, R. Benedek, and W. E. King, Phys. Rev. Lett. **59**, 1930 (1987).
[15] D. E. Alexander and G. S. Was, Phys. Rev. B **47**, 2983 (1993).
[16] J. Yan, Z. Li, C. Bai, W. S. Yang, Y. Wang, W. Zhao, Y. Kang, F. C. Yu, P. Zhai, and X. Tang, Appl. Phys. Lett. **75**, 1390 (1994).
[17] T. J. Colla, R. Aderjan, R. Kissel, and H. M. Urbassek, Phys. Rev. B **62**, 8487 (2000).
[18] K. Nordlund, K. O. E. Henriksson, and J. Keinonen, Phys. Rev. Lett. **79**, 3624 (2001).
[19] E. M. Bringa, E. Hall, R. E. Johnson, and R. M. Papaleo, Nucl. Instrum. Methods Phys. Res. B **193**, 734 (2002).
[20] E. M. Bringa and R. E. Johnson, Nucl. Instrum. Methods Phys. Res. B **193**, 365 (2002).
[21] T. van Dillenm, A. Polman, W. Fukarek, and A. van Blaaderen, Appl. Phys. Lett. **78**, 910 (2001).
[22] A. Berthelot, F. Gourbilleau, C. Dufour, B. Domenges, and E. Paumier, Nucl. Instrum. Methods Phys. Res. B **166**, 927 (2000).
[23] H. H. Andersen, H. Knudsen, and P. Moller Petersen, J. Appl. Phys. **49**, 5638 (1978).
[24] D. E. Alexander, G. S. Was, and L. E. Rehn, J. Appl. Phys. **70**, 1252 (1991).
[25] H. A. Atwater, C. V. Thompson, and H. I. Smith, J. Appl. Phys. **64**, 2337 (1988).
[26] K. Sekar, P. V. Satyam, G. Kuri, D. P. Mahapatra, and B. N. Dev, Nucl. Instrum. Methods Phys. Res. B **73**, 63 (1993).
[27] GATAN Inc., USA